Check for updates

HIP25 special issue

I·M3 Institute of Materials, Minerals & Mining

Powder Metallurgy
1–6
© The Author(s) 2026

Article reuse guidelines:
sagepub.com/journals-permissions
DOI: 10.1177/00325899261454821
journals.sagepub.com/home/pmg

Sage

Accelerated fatigue testing of powder metallurgical HIP high-speed steel for near-net shape applications

Leonhard Gertlowski[1,2], Oliver Schenk[2], Stefan Müller[3], Santiago Benito[3], Sebastian Weber[3] and Christoph Broeckmann[1,2]

Abstract

High-speed steels are commonly used for cutting tools requiring a high impact toughness and fatigue resistance. Both properties are significantly enhanced by employing the powder metallurgical (PM) production route using HIP as consolidation technique. However, the inherent oxides of the used powder may reduce the fatigue limit. Hence, subsequent forging is commonly required, which in turn precludes the possibility of near net shape production by PM. The purpose of this study is to investigate the efficiency of an isothermal holding stage that is introduced prior to the application of pressure to allow oxide size reduction during the HIP process and thereby increasing fatigue limit. The fatigue limit is assessed by accelerated fatigue testing, allowing its determination with a single specimen, which is particularly crucial for HIP processes with limited capsule volume. Good agreement is observed with results from conventional fatigue testing based on the staircase method.

Keywords

high-speed steel, accelerated fatigue testing, near net shape, oxide network, heat treatment, forging

Received: 12 August 2025; accepted: 13 May 2026

Introduction

High-speed steels (HSSs) constitute a group of high-alloy steels that contain tungsten, molybdenum, vanadium, cobalt and chromium as essential alloying elements, in addition to iron and carbon. The primary carbides and eutectic carbides embedded in the martensitic matrix ensure excellent wear resistance, while the fine tempering carbides contribute to a high hot hardness. HSS are commonly used for cutting tools that require a high impact toughness and fatigue resistance. Both properties are significantly enhanced by using powder metallurgical (PM) HIP as consolidation technique. PM-HIP allows the formation of both, smaller carbides and grains than in ingot cast HSS.[1–4]

However, the fatigue limit of PM-HIP HSS is adversely affected by oxide networks that form along the former powder particle boundaries.[5] According to Murakami, larger defects correlate with a lower fatigue limit.[6–9] As a result, HSS is conventionally forged in order to break up the oxide networks and reduce the size of the failure-relevant defects. Nevertheless, the forging process precludes the potential of a net shape production by PM-HIP. An encouraging methodology for integrating near-net shape production with a high fatigue limit is oxide reduction by carbothermal reaction, which implies the simultaneous formation of carbon monoxide and dioxide. This mechanism requires a favourable thermodynamic condition including a combination of a sufficiently high temperature and a fine vacuum in the absence of notable densification of the powder. Accordingly, an additional holding stage is introduced during the heating stage of the HIP process prior to consolidation. As the HIP capsule may be considered as a closed system, a removal of the oxides is not possible. Consequently, the oxides precipitate once more during the ongoing HIP cycle. However, the new oxides are expected to be of a smaller size than the original oxides, favouring higher fatigue limit.[10]

The fatigue limit is commonly assessed in a statistical manner by a systematical variation of a stress amplitude in the vicinity of the presumed load limit. This implies the cyclic loading of individual specimens with a constant stress amplitude and a predefined number of cycles N_{lim}. If the specimen is subjected to fracture, the stress amplitude is reduced for the subsequent specimen, whereas the stress amplitude is increased otherwise. This procedure is referred to as the staircase method according to Dixon and Mood.[11,12]

This method requires a considerable number of test specimens to adequately describe the stochastic failure characteristics. This is in contradiction with the use of a limited test

[1]Institute of Applied Powder Metallurgy and Ceramics at RWTH Aachen e.V., Aachen, Germany
[2]Institute for Materials Applications in Mechanical Engineering, RWTH Aachen University, Aachen, Germany
[3]Chair of Materials Technology, Ruhr University Bochum, Bochum, Germany

Corresponding author:
Leonhard Gertlowski, Institute of Applied Powder Metallurgy and Ceramics at RWTH Aachen e.V., Augustinerbach 4, 52062 Aachen, Germany; Institute for Materials Applications in Mechanical Engineering, RWTH Aachen University, Augustinerbach 4, 52062 Aachen, Germany.
Email: l.gertlowski@iwm.rwth-aachen.de

Table 1. Chemical Composition of the HS3-3-4 (1.3377) Batches.

	C [wt.%]	Si [wt.%]	Mn [wt.%]	Co [wt.%]	Cr [wt.%]	Mo [wt.%]	V [wt.%]	W [wt.%]	Fe [wt.%]	O [ppm]
As-forged	1.5	0.7	0.3	0.4	4.0	2.6	3.7	2.5	Bal.	51
As-HIPed	1.5	0.5	0.3	0.6	4.2	2.5	4.1	2.8	Bal.	113

volume, such as that available in a HIP capsule. Accordingly, accelerated fatigue testing methods have been developed to determine the fatigue limit based on the self-heating of a single specimen under cyclic loading. The stress amplitude is increased continuously throughout a single experiment after a defined number of cycles and the temperature increase induced by each load level is recorded. At stress amplitudes below the fatigue limit, as applied at the beginning of the accelerated fatigue testing, the temperature increase due to elastic hysteresis is small.[13] Once the fatigue limit is exceeded, each increase in stress amplitude leads to an initial rise in temperature, followed by stabilization at a steady-state value.[14] This temperature increase is attributed to microplastic deformation and indicates the onset of microstructural damage.[15] The steady-state temperature as a function of stress amplitude can be described by two linear approximations: one at lower load levels and one immediately before fracture. Their intersection is interpreted as the fatigue limit according to the "two-curve model."[16] Accelerated testing has already been employed in the analysis of cast iron,[17] low-alloy steel,[18] stainless steel[19,20] and aluminium alloys.[21] Nevertheless, accelerated fatigue testing is not yet established for HSSs. A key challenge arises from their fatigue behaviour, as a large fraction of the fatigue life is associated with the initiation and coalescence of microcracks, while subsequent crack growth occurs thereafter.[22] Consequently, the dissipated energy is expected to be comparatively low, which may pose challenges for the estimation of the fatigue limit using thermography-based accelerated fatigue testing. To date, only a single study has investigated this approach for HS6-5-3 and HS6-5-2.[23] The present study applies the method to HS3-3-4 and compares the fatigue limit of forged PM HSS with that of PM HSS produced by HIP with holding stage.

Materials and methods

In this study, two distinct processing techniques are employed for the fabrication of HSS specimens for fatigue testing. The first processing route entails the consolidation of gas atomized HSS powder through the utilization of HIP technology, accompanied by an additional holding stage at 950 °C for period of 1 h during the heating process. The dwell time of the consolidation stage at 1100 °C and 150 MPa is 4 h. Specimens produced by HIP with an additional holding stage will be referred to as "as-HIPed." The second group of specimens is produced by machining a round forged PM HSS rod. The specimens are extracted in a longitudinal manner with respect to the forging direction. These samples will be referred to as "as-forged."

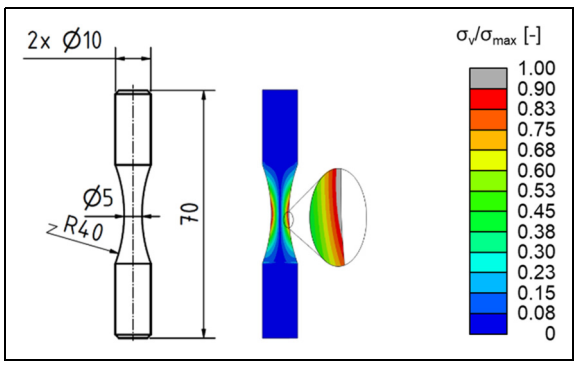


Figure 1. Geometry and stress distribution of rotating bending test specimens.

The samples are manufactured from the steel grade HS3-3-4 (1.3377) from different batches. The chemical composition is determined by optical emission spectroscopy and carrier gas hot extraction, the latter being used for oxygen analysis. The results are presented in Table 1.

The as-HIPed and as-forged specimens are machined in a soft annealed condition. Subsequently, the samples undergo a hardening process. They are austenitised at 1100 °C for 30 min and then tempered three times at 560 °C for 1 h. Thereafter, the samples are turned to the final contour and ground in the longitudinal direction.

The fatigue limit of PM HSS produced by both processing routes is evaluated through the application of conventional and accelerated fatigue testing. Conventional fatigue testing is conducted using rotating bending tests to determine the fatigue limit at a run-out of $N_{\text{lim}} = 10^7$ cycles. In total, 21 as-forged and 39 as-HIPed specimens are tested using the staircase method according to Dixon and Mood.[11] The rotating bending tests are performed on a Schenck rotating bending machine at a stress ratio of $R = -1$ and a frequency of 123 Hz. The geometry of the specimen and its stress distribution are shown in Figure 1.

The accelerated fatigue testing is conducted under axial loading with a stress ratio of $R = -1$. The temperature of the specimen is recorded, while the stress amplitude, starting at 400 MPa, is increased in steps of 20 MPa every 20,000 cycles. For temperature measurement, three negative temperature coefficient (NTC) thermistors are attached to the specimen. Temperature data are acquired at 400 ms intervals with a resolution of 0.07 °C. For insulation, a polyethylene tube is wrapped around the specimen. The accelerated fatigue tests are terminated upon specimen fracture. The geometry of the specimens and their stress distribution are shown in Figure 2. One as-forged specimen and three as-HIPed specimens are tested using accelerated fatigue testing. The as-forged specimen is tested first using a parallel gauge section with a length of 10 mm. Based on the temperature measurement obtained from this test, the length of the gauge section is increased to 20 mm for the subsequently tested as-HIPed specimens to achieve a more pronounced temperature increase. The fatigue limit is estimated using the "two-curve model," as outlined in the introduction.

The results of fatigue testing based on the staircase method and accelerated fatigue testing are compared.

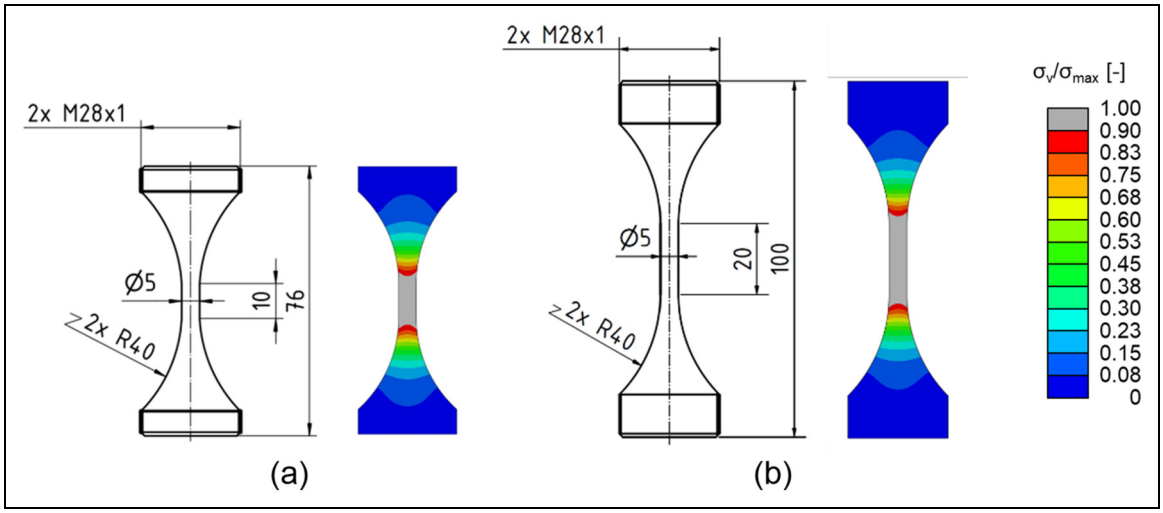


Figure 2. Geometry and stress distribution of as-forged specimens (a) and as-HIPed specimens (b) subjected to accelerated fatigue testing.

Furthermore, the fracture surfaces of as-HIPed and as-forged specimens tested under rotating bending are investigated using a *Jeol-JSM 6500* scanning electron microscope equipped with an *EDAX Microanalysis* energy dispersive spectroscopy (EDS) detector.

Results and discussion

The fatigue limit $\sigma_{A,P=50\%}$ of the as-forged samples under rotating bending was found to be 1187 MPa, whereas that of the as-HIPed samples was only 885 MPa. The S-N curves are shown in Figure 3.

The elevated fatigue limit of the as-forged samples is in agreement with the findings of the fracture surface analysis. It can be observed that the crack initiation is consistently located at an oxide for both processing routes (Figure 4). The failure-relevant oxides are smaller in the as-forged samples than in the as-HIPed samples. The mean Feret diameters are 16 ± 5 µm and 40 ± 16 µm for the as-forged and as-HIPed samples, respectively (mean $\pm$ standard deviation). The observed correlation between increased fatigue limit and smaller defect size is in accordance with the results obtained by Murakami.[6,7]

The EDS measurements of the failure-relevant defects of both the as-forged and as-HIPed samples indicate that the oxides contain elements that facilitate the formation of slag, namely aluminium, magnesium, silicon and calcium. The aforementioned oxides are inherent to the PM production route. It became evident that the large oxides could not be reduced by the additional holding stage at 950°C of the as-HIPed samples. This can be attributed to the high thermodynamic stability of alumina, magnesia, silica and calcium oxide, which precludes carbothermal reduction under the given internal capsule pressure.

The smaller oxides observed in the as-forged samples can be attributed to the fracturing of oxide networks and the subsequent crushing of the oxides during the forging process. Furthermore, the material of the as-forged samples exhibits a lower oxygen content, as indicated in Table 1. The reduced oxygen content is conducive to the formation of fewer and smaller oxides.

In addition to the fatigue testing based on the staircase method, this study also investigated accelerated fatigue testing. As an example, the temperature increase observed in an as-HIPed specimen at the end of each load level is depicted in Figure 5.

The data points at the beginning of the accelerated testing and shortly before sample fracture are approximated by two linear curves. The intersection of the two curves is interpreted as the fatigue limit.

The temperature increased by 1-2 °C until the sample fractured. The total temperature rise was significantly lower than that observed in cast iron,[17] low-alloy steel,[18] stainless steel[19,20] and aluminium alloys.[21] In contrast to cast aluminium alloys, where fatigue cracks form at an early stage and subsequent crack propagation governs most of the fatigue life,[24,25] the fatigue behaviour of HSS is dominated by the initiation and coalescence of microcracks,[22] leading to a reduced temperature rise. A comparison of the different specimens used for accelerated fatigue testing in this study, in conjunction with, Gertlowski et al.[23] indicates that an increasing highly loaded volume (HLV) relative to the surrounding, less energy-dissipating material leads to a higher temperature rise and facilitates the application of the "two-curve model."

In the present study, the fatigue limit of a HSS was successfully estimated using accelerated fatigue testing. The results of the accelerated fatigue testing and the HLVs are presented in Table 2. The HLV is defined in Equation (1) and has been determined in an FE simulation as the sum of all integration volumes V_i in which the equivalent von Mises stress $\sigma_{v,i}$ is at least 90% of the maximum stress σ_{max} within the specimen. The HLVs of the different specimen geometries are highlighted in grey in Figures 1 and 2 for rotating bending and accelerated fatigue testing, respectively.

$$\mathrm{HLV} = \sum_{\Omega_{90}} V_i, \quad \text{with } \Omega_{90} = \{ i \mid \sigma_{v,i} \geq 0.9 \cdot \sigma_{\max} \} \quad (1)$$

As already outlined in the introduction, the as-forged specimen was first tested using a parallel gauge section with a

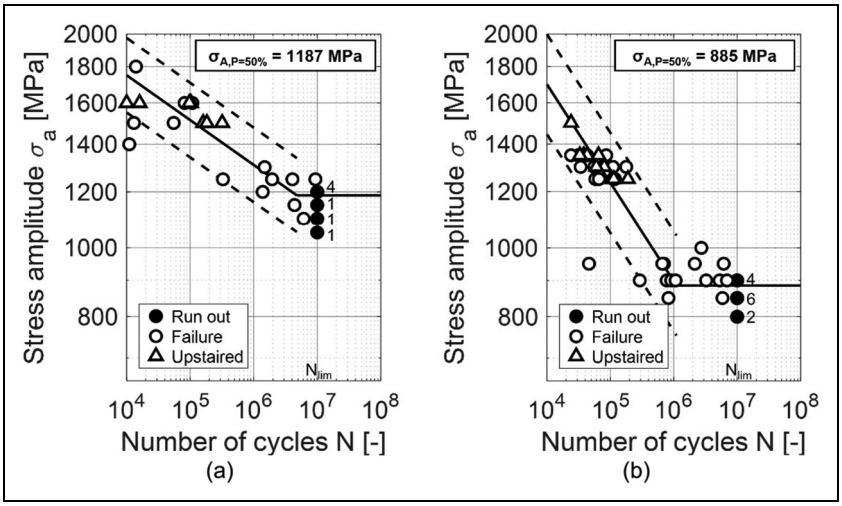


Figure 3. Statistically evaluated *S–N* curves for $\sigma_{a,P=50\%}$ (solid line) and $\sigma_{a,P=10\%}/\sigma_{a,P=90\%}$ (dashed lines): as-forged (a), as-HIPed (b).

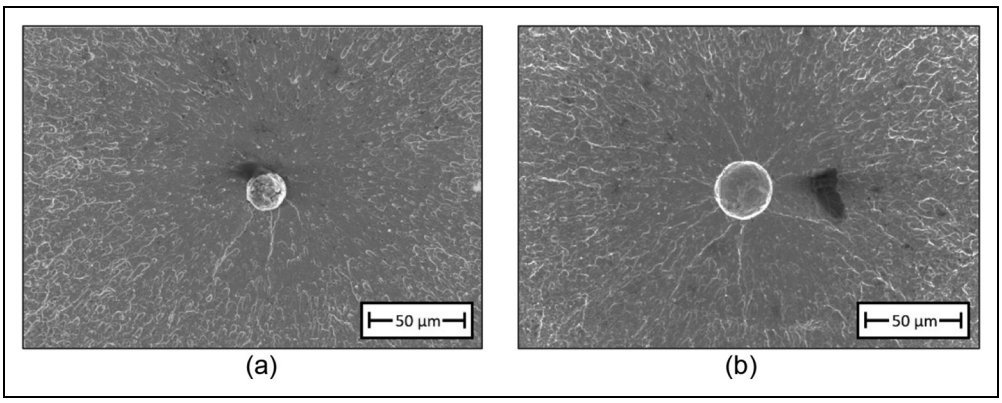


Figure 4. Fracture surfaces of rotating bending test specimens: as-forged (a), as-HIPed (b).

length of 10 mm, whereas the as-HIPed specimens were subsequently tested with a length of 20 mm. This geometric difference results in different HLVs, with the shorter gauge section of the as-forged specimen corresponding to a smaller HLV.

The estimated fatigue limit for accelerated fatigue testing is the arithmetic mean of three as-HIPed specimens and the value of one as-forged specimen. The fatigue limit determined from fatigue testing based on the staircase method is expected to be higher than that obtained from accelerated fatigue testing, since the HLV in rotating bending is considerably lower than under axial loading. By employing Equation (2), the Weibull modulus can be estimated for both the as-forged and as-HIPed samples.

$$\frac{\sigma_{\text{accelerated}}}{\sigma_{\text{staircase}}} = \left(\frac{\text{HLV}_{\text{staircase}}}{\text{HLV}_{\text{accelerated}}}\right)^{\frac{1}{m}} \quad (2)$$

A Weibull modulus of 8.3 was calculated for the as-forged samples and a value of 9.3 was obtained for the as-HIPed samples, utilizing the values provided in Table 2. It can thus be inferred that the two sample variants exhibit a comparable degree of scattering in the defect distribution. The similar degree of scatter is consistent with the comparable scatter bands of fatigue strength shown in Figure 3. This is further supported by the similar normalized standard deviations of the Feret diameters of the failure-relevant defects, indicating comparable variability in defect size between both sample conditions.

As previously stated, the temperature increase during the accelerated fatigue testing of HSS is relatively low. Consequently, it is imperative that the test setup for accelerated testing of HSS is adapted in such a way that the heat released in the HLV is dissipated as slowly as possible. In order to achieve the aforementioned objective, it is essential to insulate the sample from the surrounding atmosphere and the machine bed with an appropriate insulating material. Furthermore, the sample clamping must be as small as possible, while ensuring that the sample itself does not fracture in the area of the clamping.

Conclusion

In this study, the fatigue limit of a HSS was successfully estimated using accelerated fatigue testing and compared with the results obtained from conventional fatigue testing based on the staircase method. The temperature was measured in the parallel gauge section of the specimens under axial loading using NTCs. It was found that the temperature increase was relatively low, indicating the necessity for careful consideration of the insulation of the sample and the design of

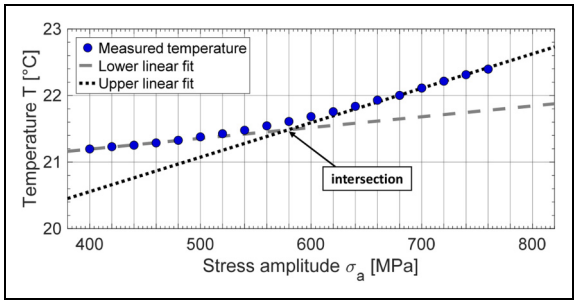


Figure 5. Temperature recorded in the parallel gauge section during accelerated fatigue testing under axial loading for an as-HIPed specimen.

Table 2. Fatigue Limit and Highly Loaded Volume (HLV) From Fatigue Tests Based on the Staircase Method (Rotating Bending Specimens) and Accelerated Fatigue Tests (Axially Loaded Specimens).

		Staircase Method		Accelerated Fatigue Testing	
		Fatigue Limit [MPa]	HLV [mm^3]	Fatigue Limit [MPa]	HLV [mm^3]
Process route	As-forged	1187	12.5	808	301
	As-HIPed	885	12.5	594	506

the test geometry. However, the desired oxide reduction through an additional holding stage during the heating process of the HIP cycle could not be achieved. The oxides with the slag-forming elements aluminium, magnesium, silicon and calcium are thermodynamically too stable. The lower fatigue limit of the as-HIPed samples compared to the as-forged samples was consistent with the larger defect size.

Acknowledgments

The authors acknowledge the funding of the project "Influence of Integrated HIP Heat Treatments on the Microstructure and Mechanical Properties of a PM Tool Steel: Experiment and Simulation" from the German Research Foundation (Grant number: 532214230).

ORCID iDs

Leonhard Gertlowski https://orcid.org/0009-0006-5175-1121
Oliver Schenk https://orcid.org/0009-0007-7263-3252
Stefan Müller https://orcid.org/0009-0005-3221-3726

Funding

The authors disclosed receipt of the following financial support for the research, authorship, and/or publication of this article: This research was funded within the project "Influence of Integrated HIP Heat Treatments on the Microstructure and Mechanical Properties of a PM Tool Steel: Experiment and Simulation" by the German Research Foundation (Deutsche Forschungsgemeinschaft) (Grant number: 532214230).

Declaration of conflicting interests

The authors declared no potential conflicts of interest with respect to the research, authorship, and/or publication of this article.

Data availability

Data will be made available on request.

References

1. Komanduri R. *Cutting-tool materials. In: encyclopedia of materials: science and technology*. Elsevier, 2001; pp. 1–13. DOI: 10.1016/B0-08-043152-6/00353-3.
2. Boccalini M and Goldenstein H. Solidification of high speed steels. *Int Mate- Rev* 2001; 46: 92–115.
3. Disch N, Benito S, Röttger A, et al. Influence of heat treatment parameters on the carbide morphology of PM high-speed steel HS 6-5-3-8. *Steel Res Int* 2023: 94. DOI: 10.1002/srin.202200755
4. Wulbieter N, Pöhl F and Theisen W. Influence of hot hardness and microstructure of high-alloyed powder metallurgical tool steels on abrasive wear behavior at elevated temperatures. *Steel Res Int* 2020: 91. DOI: 10.1002/srin.201900461
5. Scholl LM, Bezold A and Broeckmann C. Influences of manufacturing-related micro-structural variations on fatigue in carbide-rich tool steels. *Steel Res Int* 2023: 94. DOI: 10.1002/srin.202200578
6. Murakami Y, Kodama S and Konuma S. Quantitative evaluation of effects of non-metallic inclusions on fatigue strength of high strength steels. I: basic fatigue mechanism and evaluation of correlation between the fatigue fracture stress and the size and location of non-metallic inclusions. *Int J Fatigue* 1989; 11: 291–298.
7. Murakami Y and Usuki H. Quantitative evaluation of effects of non-metallic inclusions on fatigue strength of high strength steels. II: fatigue limit evaluation based on statistics for extreme values of inclusion size. *Int J Fatigue* 1989; 11: 299–307.
8. Murakami Y and Endo M. Effects of defects, inclusions and inhomogeneities on fatigue strength. *Int J Fatigue* 1994; 16: 163–182.
9. Murakami Y, Takagi T, Wada K, et al. Essential structure of S-N curve: prediction of fatigue life and fatigue limit of defective materials and nature of scatter. *Int J Fatigue* 2021; 146: 106138.
10. Vattur Sundaram M, Hryha E, Chasoglou D, et al. Effect of density and processing conditions on oxide transformations and mechanical properties in Cr–Mo-alloyed PM steels. *Metall Mater Trans A* 2022; 53: 640–652.
11. Dixon WJ and Mood AM. A method for obtaining and analyzing sensitivity data. *J Am Stat Assoc* 1948; 43: 09.
12. Pollak R, Palazotto A and Nicholas T. A simulation-based investigation of the staircase method for fatigue strength testing. *Mech Mater* 2006; 38: 1170–1181.
13. Fargione G. Rapid determination of the fatigue curve by the thermographic method. *Int J Fatigue* 2002; 24: 11–19.
14. Meneghetti G. Analysis of the fatigue strength of a stainless steel based on the energy dissipation. *Int J Fatigue* 2007; 29: 81–94.
15. Risitano A, La Rosa G, Geraci A, et al. The choice of thermal analysis to evaluate the monoaxial fatigue strength on materials and mechanical components. *Proce Instit Mech Eng, C: J Mech Eng Sci* 2015; 229: 1315–1326.

16. Cura F, Curti G and Sesana R. A new iteration method for the thermographic deter-mination of fatigue limit in steels. *Int J Fatigue* 2005; 27: 453–459.
17. Lipski A. Determination of the S-N curve and the fatigue limit by means of the ther-mographic method for ductile cast iron, Novosibirsk, Russia, 13–19 August 2018. DOI: 10.1063/1.5066398.
18. Lipski A. Determination of fatigue limit by locati methodusing S-N curve determined by means of thermographic method. *Solid State Phenomena* 2014; 223: 362–373. www.scientific.net/SSP.223.362
19. Lipski A. Thermographic method based accelerated fatigue limit calculation for steel X5CrNi18-10 subjected to rotating bending. *Pol Marit Res* 2015; 22: 64–69.
20. Lipski A. Accelerated determination of fatigue limit and S-N curve by means of thermographic method for X5CrNi18-10 steel. *Acta Mechanica et Automatica* 2016; 10: 22–27.
21. Lipski A. Rapid determination of the Wöhler's curve for aluminum alloy 2024-T3 by means of the thermographic method, Fojutowo, Poland, 17–20 May 2016. DOI: 10.1063/1.4965936.
22. Shiozawa K, Morii Y and Nishino S. Subsurface crack initiation and propagation mechanism under the super-long fatigue regime for high speed tool steel (JIS SKH51) by fracture surface topographic analysis. *JSME Int J Ser A Solid Mech Mater Eng* 2006; 49: 1–10.
23. Gertlowski L, Schenk O, Müller S, et al. Accelerated Fatigue Testing of High-Speed Steel. *Fatigue Fract Eng Mat Struct* 2026; 49: 2156–2166.
24. Zhu X, Jones JW and Allison JE. Effect of frequency, environment, and temperature on fatigue behavior of E319 cast-aluminum alloy: small-crack propagation. *Metall Mater Trans A* 2008; 39: 2666–2680.
25. Zheng X, Engler-Pinto C, Su X, et al. Correlation between scatter in fatigue life and fatigue crack initiation sites in cast aluminum alloys. *SAE Int J Mater Manf* 2012; 05: 270–276.